LAWRENCE
LIVERMORE
NATIONAL
LABORATORY

UCRL-TR-224467

Preliminary Investigations of Eddy Current Effects on a Spinning Disk

W. T. Piggott, S. Walston, D. Mayhall

September 8, 2006

Disclaimer

This work was performed under the auspices of the U.S. Department of Energy by University of California, Lawrence Livermore National Laboratory under Contract W-7405-Eng-48.

Preliminary Investigations of Eddy Current Effects on a Spinning Disk

W. Tom Piggott, Sean Walston, and David Mayhall

Introduction

The design of the positron source target for the International Linear Collider (ILC) envisions a Ti6Al4V wheel rotating in a large magnetic field (5-10 Tesla) being impacted by a photon beam to produce positrons. One of the many challenges for this system is determining how large a motor will be needed to spin the shaft. The wheel spinning in the magnetic field induces an eddy current in the wheel, which retards the spinning motion of the wheel. Earlier calculations by Mayhall [1] have shown that those eddy forces could be quite large, and resulted in the preliminary design being moved from a solid disk to a rim and spoke design, as shown in Figure 1.

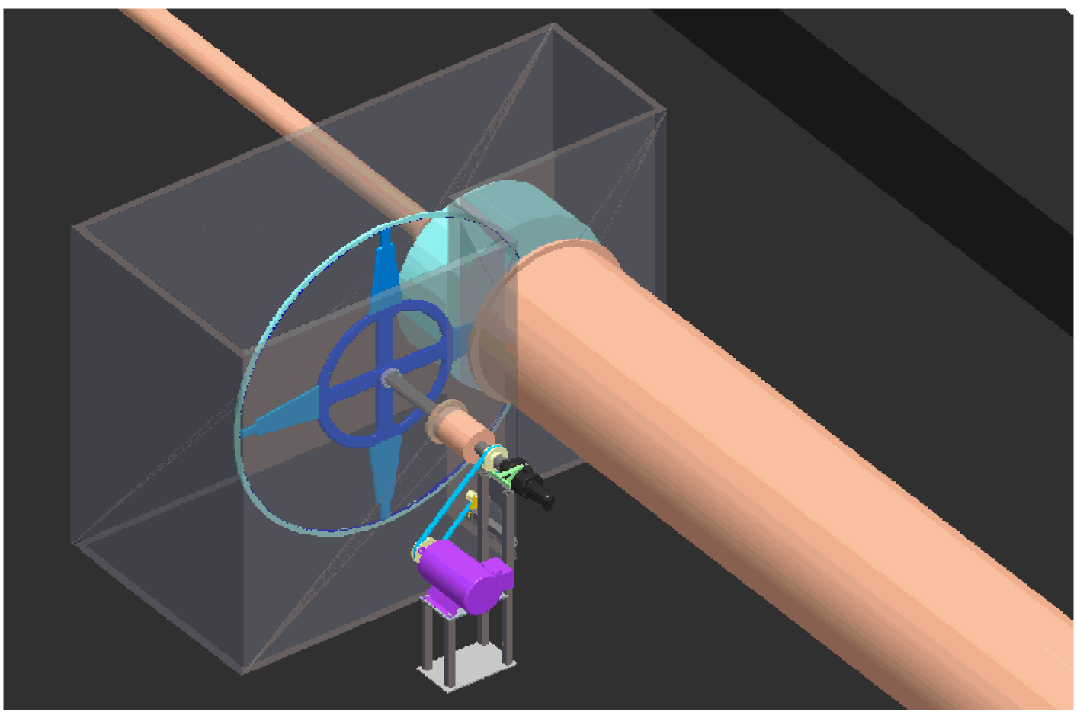

Figure 1. Rim and Spoke Target Wheel Design

A series of experiments with a spinning metal disk were run at the Stanford Linear Accelerator Center (SLAC) to provide experimental validation of the Maxwell 3D simulations. This report will give a brief outline of the experimental setup and results. In addition, earlier work by Smythe [2] will be used to compare with the experimental results.

Experimental Setup

The experiments consisted of a metal disk placed in a lathe, with a permanent magnet positioned a measured distance off the surface of the disk. The force induced on the magnet holder by the spinning disk was measured using two strain gauges – one strain gauge for the axial force, and another strain gauge for the tangential and radial forces. A picture of the setup can be seen in Figure 2. Two disks were used, a copper disk (pure vacuum quality billet) and an aluminum disk (unknown specific composition), with the magnet placed at three axial positions off the disk face: 0.01 in, 0.05 in, and 0.10 in. The Cu disk had a diameter of 9.00 in and a thickness of 0.9 in, while the Al disk had a diameter of 10.0 in and a thickness of 1.0 in. The magnet was placed 4.07 in off the axis of rotation of the spinning disks. The rate of rotation was measured optically, using the white marking on the disk rim as shown in Figure 2. The strain gauges were calibrated using various test masses ranging in weight from ~1 lb to ~3 lbs.

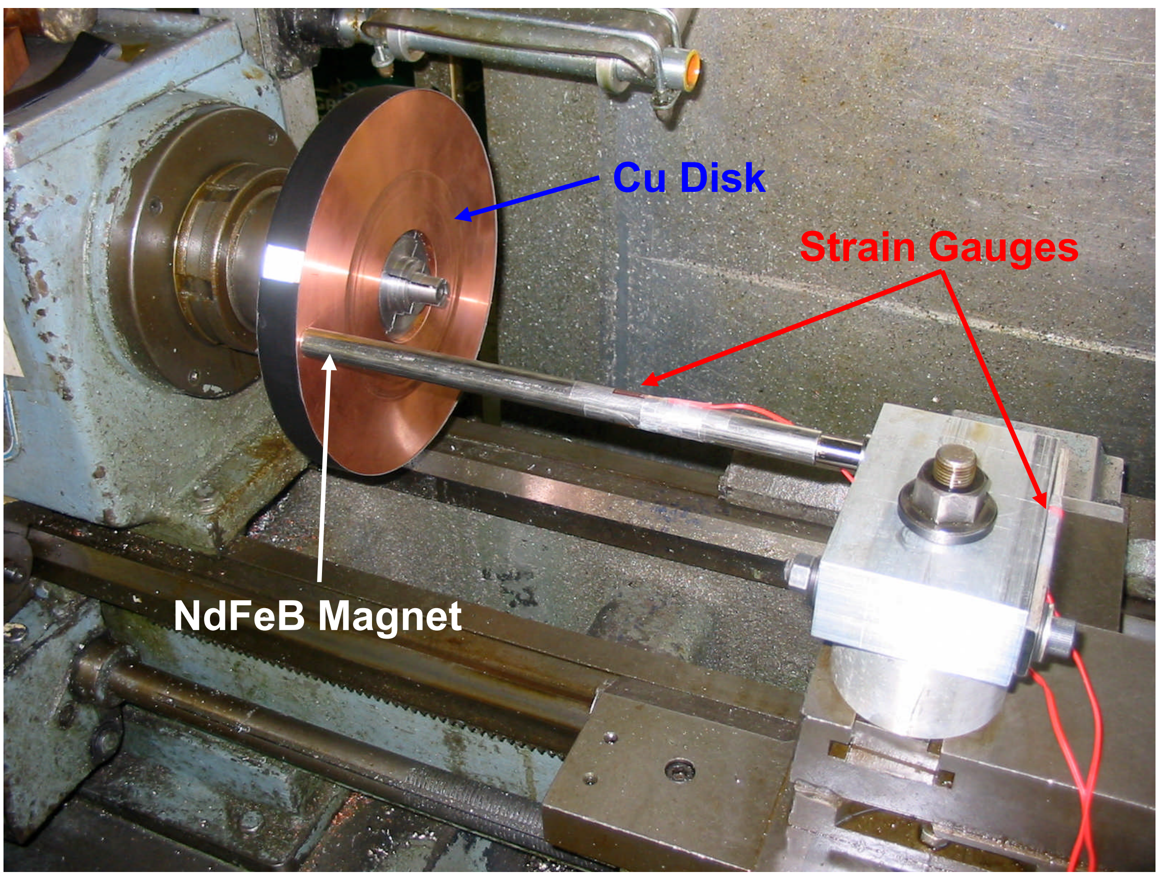

Figure 2. Experimental Setup

The magnet shop at SLAC provided a detailed map of the magnetic field from the permanent magnet stack and is shown in Figure 3.

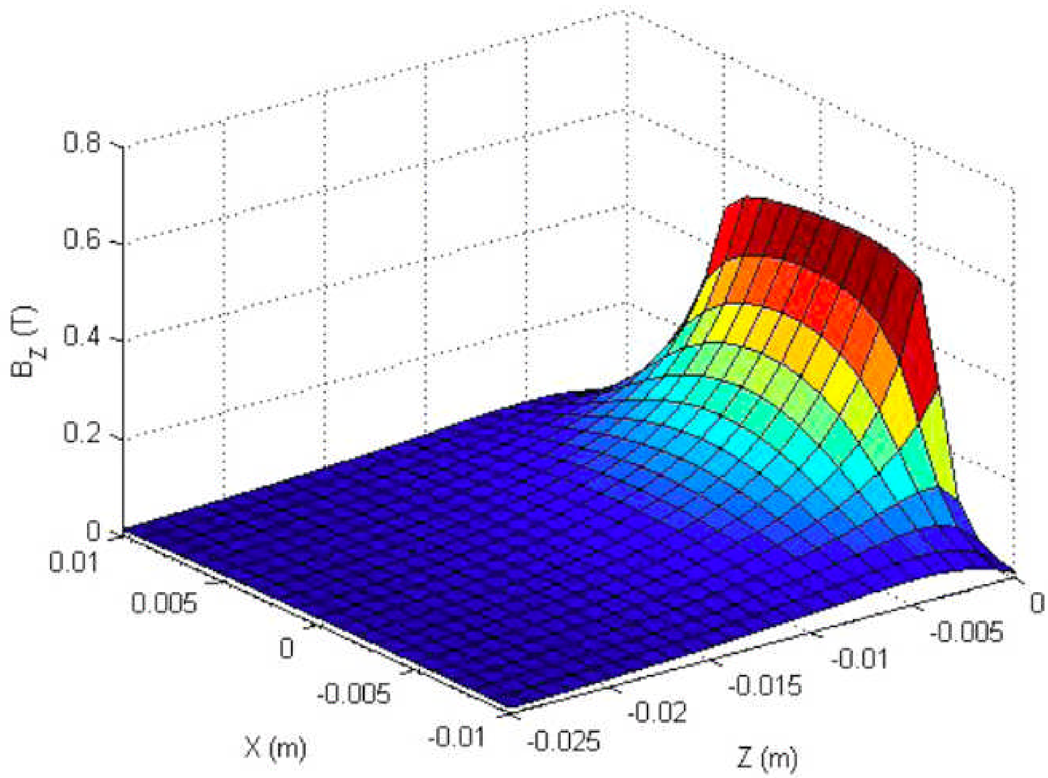

Figure 3. Permanent Magnet Field Map

Results

The raw experimental data can be found in Appendix 1. The results for the axial and tangential force versus rotational speed for the 6 experimental setups (2 disks, 3 magnet positions) can be seen in Figures 4 and 5. In addition, a pair of graphs are presented from Maxwell 3D simulations of the copper disk with 0.01 inch spacing, and can be seen in Figures 6 and 7. In addition, the field map could not be completely approximated in Maxwell 3D, and the field used in the calculations can be seen in Figure 8.

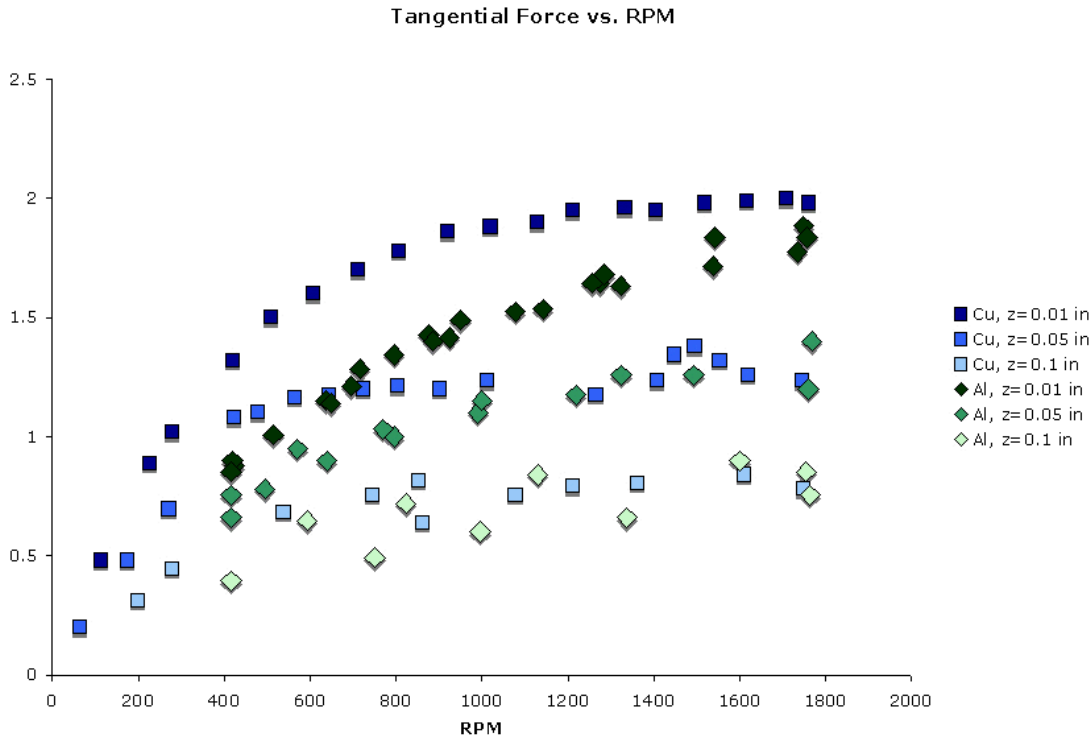

Figure 4. Tangential Force (lbs) vs. Rotational Speed

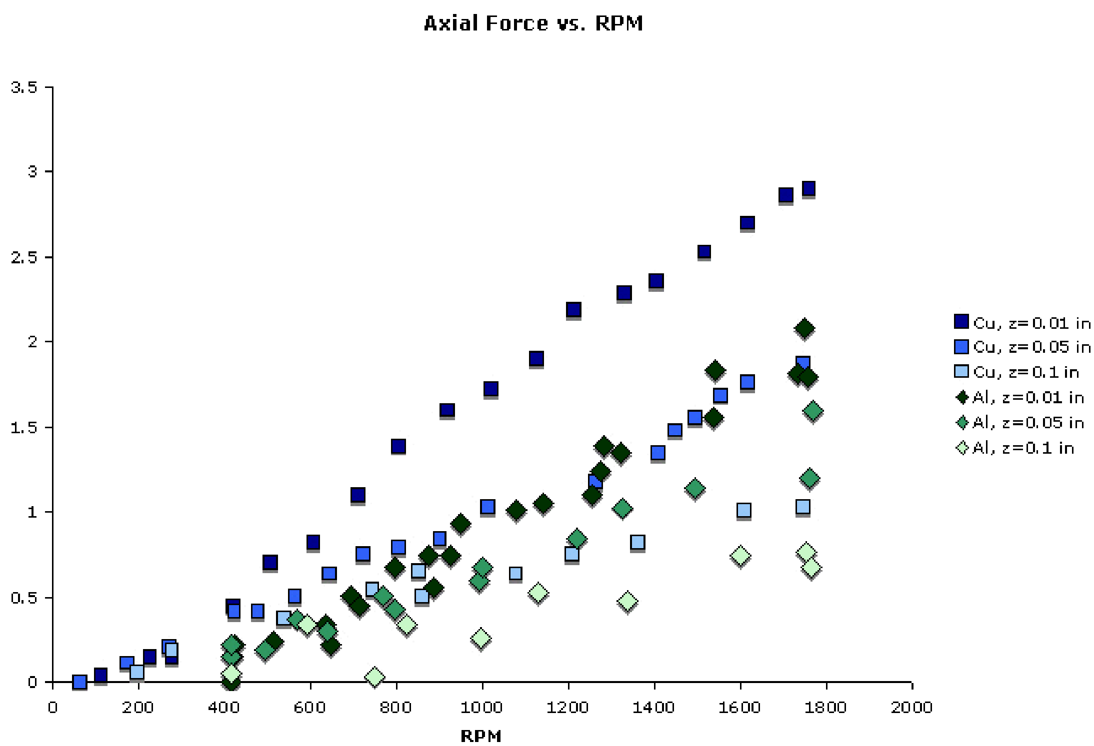

Figure 5. Axial Force (lbs) vs. Rotational Speed

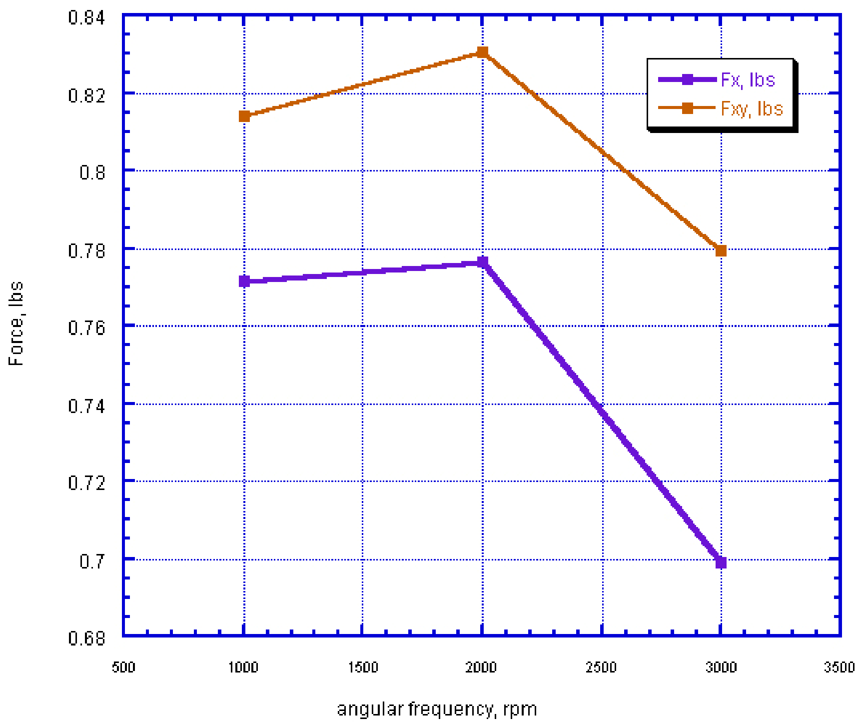

Figure 6. Force on Copper Disk, Maxwell 3D simulation, 0.01 inch spacing, 92,024 Tetrahedral Elements, Fx is tangential force, Fxy resultant force on magnet

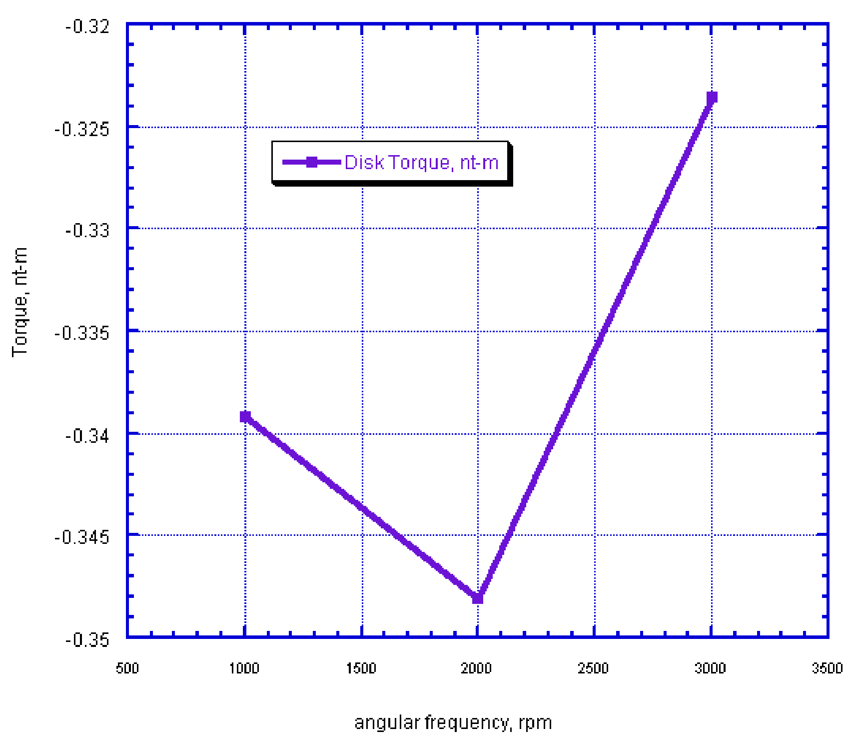

Figure 7. Torque on Copper Disk, Maxwell 3D simulation, 0.01 inch spacing, 92,024 Tetrahedral Elements

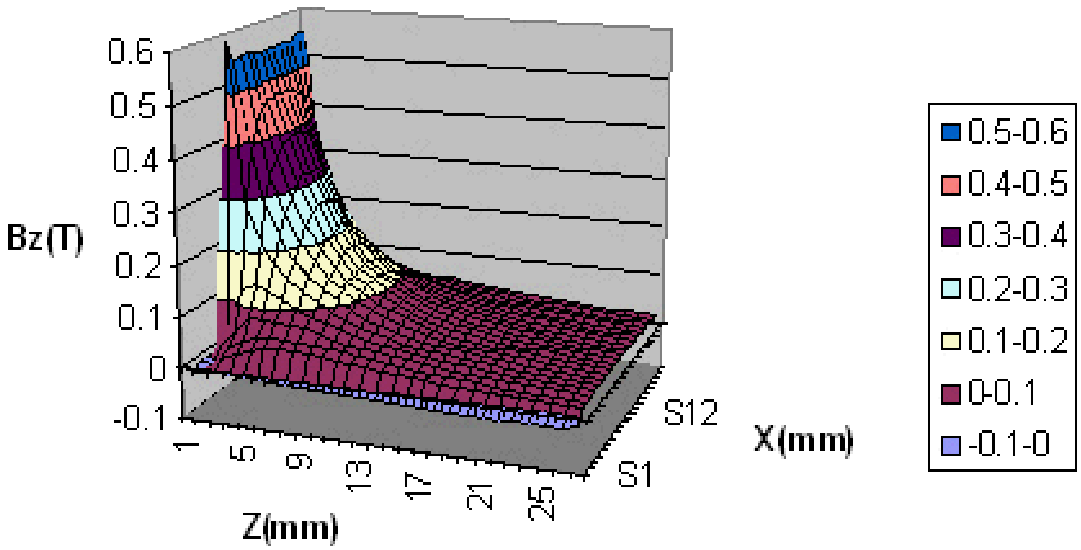

Figure 8. Magnetic Field used in Maxwell 3D calculations

A noticeable difference between the experiments and simulations is the peak and then drop in the torque and force seen in the simulations. A similar phenomenon was predicted by Smythe [2], however at very different values, as seen in Figure 9. It should be noted that there is some uncertainty regarding certain assumptions and some of the parameter values using Smythe's formulas. However, as seen in Figure 10 there is little agreement between the simulations, experimental data, and Smythe's formulas.

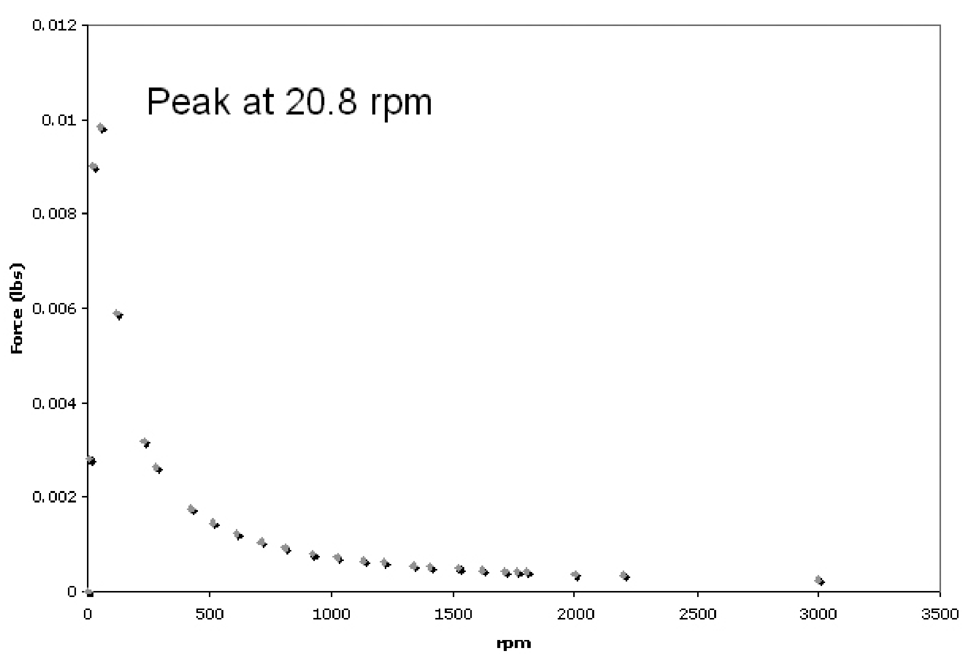

Figure 9. Force Predictions using Smythe's Formulas

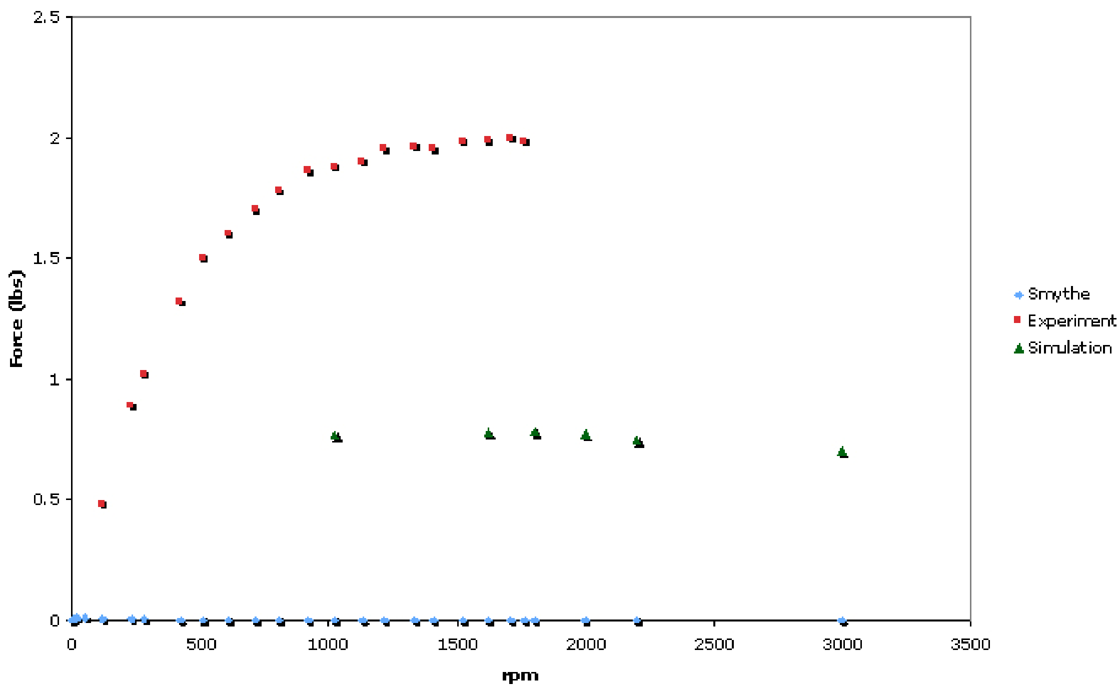

Figure 10. Force Comparison between Maxwell 3D Simulations, Experiment, and Smythe

Conclusion

Little agreement has been seen between the experiments and simulations carried out to this point. Reasonable paths forward could consist of improving the fidelity of both experiments and simulation. The experiments could be done with more instrumentation, including a torque measurement on the rotating shaft spinning the wheel. Simulations done with a greater mesh density could result in improved results. A better characterization of the materials and fields involved, including more closely approximating the actual magnetic field map in the simulation, could also result in better agreement between experimental data and simulation results. Also, there are a variety of options within the simulation that can be included, such as the eddy current effects in the permanent magnet and its holder, for example. In addition, the Smythe calculations could show different results if more appropriate values for various parameters were obtained. Even though the data do not agree currently, there are several ways to improve this result in the future.

References

1) Mayhall, David, Werner Stein, and Jeff Gronberg. Computer Calculations of Eddy-Current Power Loss in Rotating Titanium Wheels and Rims in Localized Axial Magnetic Fields. UCRL-TR-221440.
2) Smythe, W.R.. On Eddy Currents in a Rotating Disk. *AIEE Transactions*. Vol. 61, September 1942, pgs. 681-684.

Appendix. Force Raw Data
Note: All Forces in Lbs.

Below are the raw data from the spinning disk experiments. The *x* and *y* distance from the center of the magnet face to the axis of rotation was determined using the tool stock on the lathe , as was the distance *z* from the magnet face to the surface of the disk. Only *z* was changed from run to run. The data acquisition system used can only be described as prehistoric: To wit, look at the reading on the strain gauges and type the reading for the forces into a spreadsheet.

Some measuredments were made of the radial force on the magnet as well, but they were all zero to within the uncertainty on the measurement.

	measured		strain gauge
Test mass (lbs)	1.0		0.924
Center of magnet to axis, y (in)		0.75875	
Center of magnet to axis, x (in)		4	
Center of magnet to axis, r(in)		4.071326757	
Copper Disk			
Disk Thickness (in)		0.9	
Disk Radius (in)		4.5	
Magnet face to disk surface, z (in)		0.01	
rpm (actual)	Tangential Force (lbs) (direction of rotation)		Axial Force (lbs)
116		0.48	0.038
229		0.888	0.15
280		1.02	0.15
422		1.32	0.45
510		1.5	0.7
610		1.6	0.825
712		1.7	1.1
807		1.78	1.39
922		1.86	1.6
1022		1.88	1.72
1130		1.9	1.9
1214		1.95	2.19
1334		1.96	2.29
1406		1.95	2.36
1519		1.98	2.53
1618		1.99	2.7
1710		2	2.86
1762		1.98	2.9
Magnet face to disk surface, z (in)		0.05	
rpm (actual)	Tangential Force (lbs) (direction of rotation)		Axial Force (lbs)
1747		1.236	1.875
1620		1.26	1.762
1555		1.32	1.687

1497	1.38	1.556
1450	1.344	1.481
1410	1.236	1.35
1266	1.176	1.18
1015	1.236	1.032
904	1.2	0.844
806	1.212	0.788
725	1.2	0.75
645	1.176	0.638
566	1.164	0.507
480	1.104	0.413
425	1.08	0.413
65	0.2	0
177	0.48	0.113
273	0.696	0.206

Magnet face to disk surface, z (in) 0.1

rpm (actual)	Tangential Force (lbs) (direction of rotation)	Axial Force (lbs)
200	0.312	0.056
280	0.444	0.188
540	0.684	0.375
747	0.756	0.544
854	0.816	0.656
864	0.64	0.507
1080	0.756	0.638
1212	0.792	0.75
1362	0.804	0.825
1612	0.84	1.013
1750	0.78	1.032

Aluminum Disk
Disk Thickness (in) 1.0
Disk Radius (in) 5.0

Magnet face to disk surface, z (in) 0.01

rpm (actual)	Tangential Force (lbs) (direction of rotation)	Axial Force (lbs)
423	0.876	0.225
515	1.008	0.244
637	1.15	0.338
796	1.344	0.675
950	1.488	0.938
1142	1.536	1.05
1323	1.632	1.35
1538	1.716	1.556
1734	1.776	1.819
1274	1.644	1.238
925	1.416	0.75
696	1.212	0.507

420	0.9	0.15
716	1.284	0.45
877	1.428	0.75
1078	1.524	1.013
1284	1.68	1.388
1542	1.836	1.838
1749	1.884	2.081
1756	1.836	1.8
1257	1.644	1.1
887	1.4	0.56
648	1.14	0.225
417	0.852	0

Magnet face to disk surface, z (in) 0.05

rpm (actual)	Tangential Force (lbs) (direction of rotation)	Axial Force (lbs)
417	0.66	0.15
495	0.78	0.188
640	0.9	0.3
796	1	0.43
992	1.1	0.6
1218	1.176	0.844
1493	1.26	1.14
1768	1.4	1.6
1760	1.2	1.2
1325	1.26	1.03
1000	1.152	0.675
770	1.032	0.506
571	0.948	0.375
417	0.756	0.225

Magnet face to disk surface, z (in) 0.1

rpm (actual)	Tangential Force (lbs) (direction of rotation)	Axial Force (lbs)
417	0.396	0.056
594	0.648	0.337
823	0.72	0.337
1130	0.84	0.525
1600	0.9	0.75
1754	0.852	0.769
1764	0.756	0.675
1338	0.66	0.48
996	0.6	0.263
751	0.492	0.038

Magnet face to disk surface, z (in) 0.01

rpm (actual)	Tangential Force (lbs) (direction of rotation)	Axial Force (lbs)
716	1.284	0.45
877	1.428	0.75
1078	1.524	1.013

1284	1.68	1.388
1542	1.836	1.838
1749	1.884	2.081
1756	1.836	1.8
1257	1.644	1.1
887	1.4	0.56
648	1.14	0.225
417	0.852	0